

Universality in two-dimensional Kardar-Parisi-Zhang growth

F. D. A. Aarão Reis

*Instituto de Física, Universidade Federal Fluminense,
Avenida Litorânea s/n, 24210-340 Niterói RJ, Brazil
(February 2, 2008)*

We analyze simulations results of a model proposed for etching of a crystalline solid and results of other discrete models in the 2 + 1-dimensional Kardar-Parisi-Zhang (KPZ) class. In the steady states, the moments W_n of orders $n = 2, 3, 4$ of the heights distribution are estimated. Results for the etching model, the ballistic deposition (BD) model and the temperature-dependent body-centered restricted solid-on-solid model (BCSOS) suggest the universality of the absolute value of the skewness $S \equiv W_3/W_2^{3/2}$ and of the value of the kurtosis $Q \equiv W_4/W_2^2 - 3$. The sign of the skewness is the same of the parameter λ of the KPZ equation which represents the process in the continuum limit. The best numerical estimates, obtained from the etching model, are $|S| = 0.26 \pm 0.01$ and $Q = 0.134 \pm 0.015$. For this model, the roughness exponent $\alpha = 0.383 \pm 0.008$ is obtained, accounting for a constant correction term (intrinsic width) in the scaling of the squared interface width. This value is slightly below previous estimates of extensive simulations and rules out the proposal of the exact value $\alpha = 2/5$. The conclusion is supported by results for the ballistic deposition model. Independent estimates of the dynamical exponent and of the growth exponent are $1.605 \leq z \leq 1.64$ and $\beta = 0.229 \pm 0.005$, respectively, which are consistent with the relations $\alpha + z = 2$ and $z = \alpha/\beta$.

PACS numbers: 05.40.-a, 05.50.+q

I. INTRODUCTION

Surface growth processes and deposition of thin films have attracted much interest from the technological point of view [1–3] and motivated the proposal of continuum and discrete models for surface and interface growth, which also play an important role in the field of non-equilibrium Statistical Mechanics. One of the most important phenomenological theories is that of Kardar, Parisi and Zhang (KPZ) [4], in which the time evolution of the interface described by the height function h at position \vec{x} and time t is given by the KPZ equation

$$\frac{\partial h}{\partial t} = \nu \nabla^2 h + \frac{\lambda}{2} (\nabla h)^2 + \eta(\vec{x}, t). \quad (1)$$

Here ν represents a surface tension, λ represents the excess velocity and η is a Gaussian noise [2,4] with zero mean and variance $\langle \eta(\vec{x}, t) \eta(\vec{x}', t') \rangle = D \delta^d(\vec{x} - \vec{x}') \delta(t - t')$, where d is the dimension of the substrate.

The interface width $\xi(L, t) = \langle \overline{h^2} - \bar{h}^2 \rangle^{1/2}$ characterizes the roughness of the interface, for growth in a substrate of length L (overbars denote spatial averages and angular brackets denote configurational averages). For short times, the interface width scales as

$$\xi \sim t^\beta, \quad (2)$$

with β called the roughness exponent. For long times, a steady state is attained and the width saturates at

$$\xi_{sat} \sim L^\alpha, \quad (3)$$

with α called the roughness exponent. Eqs. (2) and (3) correspond to limits of the dynamical scaling relation of Family and Vicsek [5]

$$\xi \approx L^\alpha f(tL^{-z}), \quad (4)$$

where the dynamical exponent $z = \alpha/\beta$ characterizes the crossover from the growth regime to the steady state. Galilean invariance gives $\alpha + z = 2$ for KPZ in all dimensions [2,3]. The exact scaling exponents are known in $d = 1$, but no exact value was already obtained in two or more dimensions [2,3].

Many discrete models fall into the KPZ class, such as the restricted solid-on-solid (RSOS) model of Kim and Kosterlitz [6] and ballistic deposition (BD) [7]. Numerical estimates of the scaling exponents in $d = 1$ are consistent

with the exact values [6,8,9] and simulations in $d = 2$ are frequently used to estimate them. Most of the reported values of α range from $\alpha = 0.37$ to $\alpha = 0.4$ [6,10–13], which is confirmed by numerical solutions of the KPZ equation [14–17].

In 1998, assuming certain properties of the height correlation functions, Lässig obtained a quantization condition for the KPZ exponents which gave $\alpha = 2/5$ as the only solution consistent with the range of numerical estimates [18]. Another consequence of his work was that the moments of the steady state height distribution,

$$W_n \equiv \left\langle (h - \bar{h})^n \right\rangle, \quad (5)$$

would obey power-counting, i. e. they would scale as $W_n \sim L^{n\alpha}$. The second moment is the squared interface width ξ^2 . Moreover, the validity of his assumptions requires that the steady state distribution is skewed (non-zero third moment), contrary to the one-dimensional case (Gaussian distribution).

Recent numerical results of Chin and den Nijs for the RSOS and the body-centered solid-on-solid (BCSOS) models were consistent with $\alpha = 0.4$ [19], but extensive simulations of Marinari et al for the RSOS model rule out that value [20]. A recent study of the KPZ equation in the mode-coupling approximation provided an estimate $z \approx 1.62$ in $d = 2$ [21]. Despite this controversy, various works [19,20,22] confirm the power-counting property for models with restricted height differences (RSOS, BCSOS) and suggest that the skewness

$$S \equiv \frac{W_3}{W_2^{3/2}} \quad (6)$$

and the kurtosis

$$Q \equiv \frac{W_4}{W_2^2} - 3 \quad (7)$$

are universal at the steady state. According to Chin and den Nijs, these universal values do not depend on the sign of the coefficient λ of the nonlinear term of the KPZ equation (1).

Consequently, the value of KPZ exponents in $d = 2$ is still an open question, and the universality of the values of the skewness and the kurtosis deserves to be tested in models other than those with restricted height differences. The main contribution of this paper is the analysis of simulations results of a recently proposed model for etching of crystalline solids [23] which belongs to the KPZ class. Additional support to some of our conclusions will be provided by simulations results of ballistic deposition and of the temperature-dependent BCSOS model [19]. For the etching model, we will obtain $\alpha \approx 0.38$ after a detailed analysis of finite-size corrections. Characteristic relaxation times will be calculated independently and will provide estimates of the dynamical exponent $z > 1.6$, while estimates of the growth exponent give $\beta \approx 0.23$. Although our error bars intercept those obtained from extensive simulations of the RSOS model [20], our central estimates of α are smaller and, consequently, more distant from the theoretically proposed value $\alpha = 0.4$ [18]. On the other hand, our estimates are near those by Colaiori and Moore [21] from renormalization under the mode-coupling approximation. We will also show that our data for various models confirm the universality of the steady state skewness and kurtosis. Concerning the steady state skewness, although its absolute value is universal, its sign changes with the nonlinear coefficient λ of the KPZ equation.

This paper is organized as follows. In Sec. II we briefly describe the models, the simulation procedure, the methods to estimate W_n and the method to calculate characteristic relaxation times. In Sec. III, we analyze the skewness and the kurtosis at the steady states. In Sec. IV, we analyze the finite-size estimates of the scaling exponents of the etching model, also showing some results for BD. In Sec. V we summarize our results and present our conclusions.

II. MODELS AND SIMULATION PROCEDURE

The model for etching of a crystalline solid of Mello et al [23] is illustrated in Fig. 1 in its growth version. The solids have square and simple cubic lattice structures in $1 + 1$ and $2 + 1$ dimensions, respectively. At each growth attempt, a column i , with current height $h(i) \equiv h_0$, is randomly chosen. Then its height is increased by one unit ($h(i) \rightarrow h_0 + 1$) and any neighboring column whose height is smaller than h_0 grows until its height becomes h_0 . One time unit corresponds to L^2 growth attempts in $2 + 1$ dimensions. In the true etching version of this model, the columns' heights decrease by the same quantities above. However, in this paper we will always refer to the growth version of Fig. 1 as "the etching model".

In the ballistic deposition (BD) model, particles are sequentially released from randomly chosen positions above the substrate, follow a trajectory perpendicular to the surface and stick upon first contact with a nearest neighbor occupied site [2,7].

In the BCSOS model defined by Chin and den Nijs [19], the substrate is a square lattice and the heights h in the first (second) sublattice are restricted to assume even (odd) values. Also, the nearest neighbor columns always differ in height by $\Delta h = \pm 1$. The energy of a given heights configuration $\{h\}$ is given by $E(\{h\}) = \sum_{\langle i,j \rangle} \frac{1}{4} K (h_i - h_j)^2$, where K is an inverse temperature parameter and the sum runs over all next nearest neighbor pairs. At each deposition attempt, a column c is randomly chosen and, if the constraint of the heights difference is satisfied, then $h(c) \rightarrow h(c) + 2$ with probability $p \equiv \min(1, \exp(-\Delta E))$, where ΔE is the energy change if the deposition takes place. The corresponding coefficient λ (Eq. 1) changes sign at a critical point K_c [19,24].

The etching model was simulated in lattices of lengths $L = 2^n$ ($n = 5$ to $n = 10$) and lattices of lengths $L = 2^m \times 50$ ($m = 0$ to $m = 4$). The maximum deposition time ranged from 10^3 for the smallest lattices to 6×10^4 for the largest ones. During half of this time or more, the systems have undoubtedly attained their steady states. For the smallest lattices, 2×10^4 realizations were simulated, and nearly 300 realizations for the largest lattices ($L = 800$ and $L = 1024$). BD was simulated in lattices of lengths $L = 2^n$, from $n = 5$ ($L = 32$) to $n = 11$ ($L = 2048$). For the analysis of the skewness and of the kurtosis, it was essential to simulate this model in very large lattices, thus the number of realizations was relatively small: typically 10^3 realizations for $L \leq 512$, 35 for $L = 1024$ and 8 for $L = 2048$. The temperature-dependent BCSOS model was simulated with $K = 0.25$ ($L = 16$ to $L = 128$) and $K = 1.0$ ($L = 16$ to $L = 512$). For $L \leq 256$, 10^3 different realizations were considered, and 40 realizations for $L = 512$.

The procedure to calculate average quantities, described below, followed the same lines for all models. It was previously used in the analysis of other growth models in $1+1$ and $2+1$ dimensions [9,26,27].

One important point is the criterion to determine the initial time t_{min} for estimating average quantities at the steady state. In this regime, the interface width ξ fluctuates around an average value instead of increasing systematically, which was the case in the growth and in the crossover regions. Thus, for a fixed lattice length L , the first step was choosing a time interval $t_{min} \leq t \leq t_{max}$, with nearly constant ξ , from visual inspection of the $\xi \times t$ plot (t_{max} was always the maximum simulation time). Subsequently, two tests were performed. For the first test, the interval was divided in 5 subintervals and the average value of ξ was calculated in each one, forming a sequence of estimates $\{\xi(i)\}$, with $i = 1, \dots, 5$. If $\xi(i) < \xi(i-1)$ at least two times along this sequence, then the average value of ξ in the region $t_{min} \leq t \leq t_{max}$, ξ_{sat}^{trial} , was calculated. In the second test, from the plot of $\log(\xi_{sat}^{trial} - \xi(t)) \times t$, for t in the crossover region, we obtained a rough estimate of the characteristic time τ of relaxation to the steady state, as shown in Ref. [26]. If $t_{min} > 10\tau$, then the interval $t_{min} \leq t \leq t_{max}$ was accepted as representative of the steady state. Otherwise, a larger value of t_{min} was chosen and the tests were repeated (it seldom occurred).

In order to estimate the moments of the height distribution and their error bars, we used their average values within the five subintervals defined above. Final estimates of W_n are averages of these values, and error bars were obtained from their variances.

The dynamical exponent was estimated using a recently proposed method [26], in which a characteristic time τ_0 , proportional to the relaxation time τ , is calculated. For fixed L , after calculating the saturation width $\xi_{sat}(L)$, τ_0 is defined through

$$\xi(L, \tau_0) = k \xi_{sat}(L), \quad (8)$$

with a constant $k \lesssim 1$. From relation (4), we obtain

$$\tau_0 \sim L^z. \quad (9)$$

Typically, the uncertainty in τ_0 is much smaller than that of τ , estimated from $\log(\xi_{sat} - \xi) \times t$ plots - see Ref. [26].

We estimated τ_0 with k ranging from $k = 0.5$ to $k = 0.8$. Although these constants are not much different, the values of τ_0 for $k = 0.5$ and $k = 0.8$ typically differ by a factor 4, for fixed L . This method was already applied with success to calculate the dynamical exponent of other models in various universality classes [26,27].

III. UNIVERSALITY OF SKEWNESS AND KURTOSIS

In Fig. 2a we show the steady state skewness $S(L, t \rightarrow \infty)$ of the etching model as a function of the inverse lattice length, which provides a good linear fit of the data, with an asymptotic estimate $S = 0.26 \pm 0.01$. The absolute value of S agrees with results of Chin and den Nijs [19], Shim and Landau [22] and Marinari et al [20] for the RSOS model of Kim and Kosterlitz [6] and for BCSOS models, but those authors obtained S with negative sign. Here, the positive sign is related to the presence of sharp hills (see process at the left in Fig. 1) and wide valleys at the surface of the deposit, the opposite being observed in RSOS deposits.

Note that Eq. (1) is invariant under the transformations $h \rightarrow -h$ and $\lambda \rightarrow -\lambda$, without changing the other parameters. This transformation changes the sign of the skewness. Consequently, we expect that the sign of S is related to that of λ , as previously observed in the growth regimes of 1 + 1-dimensional KPZ systems [28]. In fact, in the true etching version of this model, with erosion leading to decreasing heights, the sign of S changes, corresponding to the transformation $h \rightarrow -h$, $\lambda \rightarrow -\lambda$.

Results for the other models contribute to this discussion. In Fig. 2b we show $S(L, t \rightarrow \infty)$ versus $1/L$ for the BD model. Note that S is negative for small lattices (typically $L < 500$), but for large lattices it becomes positive, showing that there are significant morphological differences between the steady states of small lattices and those of very large systems. This is the main reason to avoid extrapolating the data in Fig. 2b, even choosing extrapolation variables other than that $1/L$ (this abscissa in Fig. 2b was chosen only for illustrate the evolution of S with L). Other consequences of this complex finite-size behavior were previously discussed in Ref. [9]. However, it is clear from Fig. 2b that S is asymptotically positive.

In Figs. 2c and 2d we show the steady state skewness for the temperature-dependent BCSOS models with $K = 0.25$ and $K = 1.0$, respectively. For $K = 0.25$, the extrapolation of the three last data points give $S = -0.28 \pm 0.015$, reinforcing the conclusion on the universality of $|S|$. Due to the small number of data points, the asymptotic correction term may be other than $1/L$, but it would not affect that conclusion. For $K = 1.0$, the skewness is always positive and rapidly increases with L , thus no extrapolation variable of the form $L^{-\Delta}$, with $\Delta > 0$, provides a reasonable linear fit. However, S will certainly converge to a positive value as $L \rightarrow \infty$, showing that the sign of the steady state skewness changes as K increases.

The sign of the corresponding parameter λ is obtained from the size dependence of the growth velocity. The steady state growth velocity, $v_s(L)$, and the velocity in an infinitely large substrate at long times, v_∞ , obey the relation [29]

$$v_s(L) = v_\infty - a\lambda L^{-\alpha_\parallel}, \quad (10)$$

where $\alpha_\parallel = 2(1 - \alpha)$ and a is positive. Considering $\alpha = 0.38$ (see Sec. IV), we obtain $\alpha_\parallel = 1.24$. In Figs. 3a-3d, we plotted $v_s(L)$ versus $x \equiv 1/L^{1.24}$ for the four models. For the etching model, the BD model and the BCSOS model with $K = 1.0$ (Figs. 3a,b,d), v_s decreases with x , which gives a positive λ , while the opposite occurs in the BCSOS model with $K = 0.25$. It confirms that the steady state skewness of the KPZ equation has the same sign of the parameter λ , its absolute value being universal. The same conclusion was derived from the time dependence of the velocity in the growth regime [29].

At this point, we recall that Chin and den Nijs [19] simulated the temperature-dependent BCSOS model with $K = -0.25$ and $K = 0.25$, obtaining $S \approx -0.26$ in both cases. They concluded that S did not depend on λ , but they did not estimate the values of this parameter. Since λ is expected to cross zero for a positive K , we conclude that their work failed to consider the regime of positive λ , which is represented here by $K = 1.0$.

Now we turn to the analysis of the kurtosis (Eq. 7). In Fig. 4a we show the steady state Q for the etching model, as a function of $1/L$. The size dependence is much weaker than that of the skewness, so that extrapolation variables other than $1/L$ do not have a significant influence on the asymptotic estimate, $Q = 0.134 \pm 0.015$ (the large error bar is mainly a consequence of the uncertainties of the finite-size data). This estimate agrees with previous ones for models with restricted heights differences [19,22,20], suggesting that the steady state kurtosis is also universal. In Fig. 4b, we show the data for the BD model and for the BCSOS model with $K = 0.25$ and $K = 1.0$, which have significant finite-size dependence (in particular those for BD). Thus, the extrapolated values have very large error bars, but are still consistent with a universal value of Q .

IV. ROUGHNESS, DYNAMICAL AND GROWTH EXPONENTS

Our first step to estimate the roughness exponent was to calculate effective exponents $\alpha_{(L,i)}$ defined as

$$\alpha_{(L,i)} \equiv \frac{\ln [\xi_{sat}(L) / \xi_{sat}(L/i)]}{\ln i}. \quad (11)$$

It is expected that $\alpha_{(L,i)} \rightarrow \alpha$ for any value of i .

Using different values of i in Eq. (11), we noticed that $\alpha_{(L,i)}$ varied with L typically in the range $0.33 \leq \alpha_{(L,i)} \leq 0.38$ for $50 \leq L \leq 1024$, which suggests that corrections to the scaling relation (3) are relevant. Our first proposal is to assume the main scaling correction as

$$\xi_{sat} \sim L^\alpha (a_0 + a_1 L^{-\Delta}), \quad (12)$$

where a_0 and a_1 are constants. Consequently, $\alpha_{(L,i)}$ is expected to vary as

$$\alpha_{(L,i)} \approx \alpha + BL^{-\Delta}, \quad (13)$$

where

$$B = \frac{(1 - i^\Delta) a_1}{\ln(i) a_0}. \quad (14)$$

Our data with $50 \leq L \leq 1024$ were analyzed using four values of i in Eq. 11: $i = 2$, $i = 2.56$, $i = 3.125$ and $i = 4$ (for noninteger i , only three or four effective exponents can be calculated). For each i , we plotted $\alpha_{(L,i)} \times L^{-\Delta}$ using several exponents Δ and did least squares fits of those plots, from which the linear correlation coefficients $r(\Delta, i)$ were obtained. Since there is no argument to predict the value of Δ , we adopted the condition of maximizing the coefficient r to extrapolate our data. In Table I, we show the exponents Δ which gave the largest r (best linear fits) for each i . The procedure is illustrated in Figs. 5a and 5b, in which we show $\alpha_{(L,2)} \times L^{-0.55}$ and $\alpha_{(L,2)} \times L^{-0.65}$, respectively, with the corresponding linear fits. The values of Δ in Figs. 5a and 5b are those which give the best fits with $i = 2$ and $i = 4$, respectively (see Table I).

Δ is expected to be independent of the particular choice of i in Eq. (11), so the differences between the estimates in Table I are effects of the maximization of r . Moreover, other exponents Δ near the values shown in Table I also provided reasonable linear fits of $\alpha_{(L,i)} \times L^{-\Delta}$ plots. In other words, large linear correlation coefficients were also obtained by considering $0.3 \lesssim \Delta \lesssim 0.8$ for different choices of i . Consequently, it is not possible to obtain a reliable estimate of that correction exponent. On the other hand, the asymptotic α obtained from the same fits fluctuate within a narrow range. Accounting for the error bars of the data, we obtained $\alpha = 0.385 \pm 0.01$ for $i = 2$ and $\alpha = 0.382 \pm 0.01$ for $i = 4$.

We also checked the effect of considering a fixed correction exponent $\Delta = 0.55$ (which is near the values in Table I) for all values of i . This procedure will be called fixed Δ method. Least squares fits of the $\alpha_{(L,i)} \times L^{-0.55}$ plots were performed, providing the slopes B which are shown in Table I. From Eq. (14), it is expected that $\frac{B \ln i}{(1-i^\Delta)} = \frac{a_1}{a_0} = \text{const}$ (see also Eqs. 12 and 13), thus we also showed in Table I the corresponding estimates of $\frac{B \ln i}{(1-i^\Delta)}$. This quantity fluctuates with i , indicating that there is no systematic trend in our results due to choice of different values of i for calculating effective exponents. Also notice that the estimates of α from the fixed Δ method are in same range of the those obtained from the maximization of correlation coefficients.

Since the range of lattice lengths considered here is not very large and the correction exponents Δ estimated above are relatively small, we tried to improve our analysis with a different assumption for the scaling corrections. Contrary to the previous procedure, now we will consider a well defined form for the main scaling correction, which is an additional constant term ξ_I^2 in the dynamic scaling relation (4) for the squared interface width:

$$\xi^2(L, t) = \xi_I^2 + L^{2\alpha} g(tL^{-z}), \quad (15)$$

where g is a scaling function. ξ_I is called intrinsic width and represents contributions of small length scales fluctuations, typical of models with large local heights differences [30–32] such as the etching model and the BD model. From Eqs. (15) and (12), the assumption of the intrinsic width as the most relevant subleading correction corresponds to a (fixed) correction exponent $\Delta = 2\alpha \approx 0.8$. It is slightly larger than the typical values obtained in the previous analysis.

Effective exponents $\alpha_L^{(I)}$ which cancel the contribution of ξ_I^2 are defined as

$$\alpha_L^{(I)} \equiv \frac{1}{2} \frac{\ln [\xi_{sat}^2(2L) - \xi_{sat}^2(L)] / [\xi_{sat}^2(L) - \xi_{sat}^2(L/2)]}{\ln 2}. \quad (16)$$

In Fig. 6a we show $\alpha_L^{(I)}$ versus $1/L$ for the etching model and a least squares fit of these data, which provides $\alpha = 0.383$ asymptotically. Here, the variable $1/L$ in the abscissa was chosen only to illustrate the behavior of the $\alpha_L^{(I)}$ data. It represents a second correction term for the ξ scaling, which is still more difficult to measure than the first correction term. Thus, we also tested other variables in the form $L^{-\Delta_1}$ to extrapolate $\alpha_L^{(I)}$, with $0.5 \leq \Delta_1 \leq 2$ ($\Delta_1 = 1$ was used in Fig. 6a). The corresponding linear fits give $0.380 < \alpha < 0.387$. The small range of the asymptotic α is a consequence of the slow variation of $\alpha_L^{(I)}$ with L (2% from $L = 100$ to $L = 500$), as shown in Figs. 6a. Accounting for the error bars of the data, our final estimate is $\alpha = 0.383 \pm 0.008$.

The forms of finite-size corrections analyzed above, Eqs. (13) and (15), cannot be rigorously justified, but are based on heuristic arguments. See e. g. Ref. [2] and references therein. Certainly, the fact that $\alpha_L^{(I)}$ increases slowly with

L is a support to the assumption that the intrinsic width is the most relevant correction term to ξ^2 . Anyway, using different assumptions on the scaling corrections was essential to confirm the reliability of the above estimate of the roughness exponent.

The universality of the values of skewness and kurtosis imply that W_3 and W_4 may also be used to estimate α . The effective exponents obtained from the third moment have very large error bars, but those obtained from the fourth moment behave similarly to the ones obtained from the interface width. The analogous of exponents $\alpha_{(L,2)}$ and $\alpha_{(L,4)}$ (Eq. 11) calculated with W_4 also converge to the range $0.38 \leq \alpha \leq 0.385$ with strong corrections to scaling. Effective exponents which cancel the contribution of a constant additive term in the dynamic scaling relation for W_4 (analogous to $\alpha_L^{(I)}$) are defined as

$$\alpha_L^{(I,4)} \equiv \frac{1}{4} \frac{\ln [W_4(2L, t \rightarrow \infty) - W_4(L, t \rightarrow \infty)] / [W_4(L, t \rightarrow \infty) - W_4(L/2, t \rightarrow \infty)]}{\ln 2}. \quad (17)$$

They are plotted in Fig. 6b as a function of $1/L$. The asymptotic estimate, obtained with the procedure described above, is $\alpha = 0.379 \pm 0.012$. It is in good agreement with the estimate from the interface width and also excludes $\alpha = 0.4$.

The same analysis was also performed with the BD model, as shown in Fig. 7, with data for $L \leq 512$. Although the results are less accurate than those for the etching model, they also suggest that $\alpha < 0.4$ asymptotically.

In order to estimate the dynamical exponent z , we calculated effective exponents z_L defined as

$$z_L \equiv \frac{\ln [\tau_0(2L) / \tau_0(L/2)]}{\ln 4}, \quad (18)$$

using the characteristic times τ_0 defined in Sec. II (Eqs. 8 and 9). In Figs. 8a and 8b we show z_L versus $1/L$ for the etching model, obtained using $k = 0.6$ and $k = 0.8$ to calculate τ_0 , respectively. Here, the abscissa $1/L$ is also chosen to illustrate the evolution of z_L , but not to perform extrapolations of the data. Although the error bar of the data for $L = 800$ is relatively large, those plots indicate that $z > 1.6$. Considering the trend for large L and different values of k , we estimate $1.605 \leq z \leq 1.64$. These values are consistent with the above estimates of α and the exact relation $\alpha + z = 2$.

Finally, we estimated the growth exponent (Eq. 2) of the etching model with the same procedure previously applied with success to BD and to the Das Sarma and Tamborenea model in $1 + 1$ dimensions [9,27]. The growth region for each L begins at $t_0 = 50$ and ends at the maximum time τ_{max} such that the linear correlation coefficient of the data in the range $t_0 \leq t \leq \tau_{max}$ exceeds a fixed value r_{min} [9]. Here, $r_{min} = 0.99995$ and $r_{min} = 0.9999$ are considered. Effective exponents β_L are defined as the slopes of the linear fits of $\log W \times \log t$ plots using all data in the above-defined growth regions. In Fig. 9 we plot β_L versus $1/L$ for the etching model using $r_{min} = 0.99995$ and $r_{min} = 0.9999$. The error bars of those effective exponents is very small. We also show in Fig. 9 the linear fits of the $\beta_L \times 1/L$ data for each r_{min} . Other variables in the form $L^{-\Delta}$ were used to extrapolate the β_L data, giving asymptotic estimates $\beta = 0.229 \pm 0.005$. Within error bars, it agrees with the value $\alpha/z = 0.234 \pm 0.009$ obtained from the above estimates of α and z .

V. CONCLUSION

We studied four $2 + 1$ dimensional discrete growth models in the KPZ class, determining critical exponents and steady state values of the skewness S and the kurtosis Q . Accurate estimates of the scaling exponents were obtained for the etching model proposed by Mello et al [23]: $\alpha = 0.383 \pm 0.008$, $1.605 \leq z \leq 1.64$, $\beta = 0.229 \pm 0.005$. Results for the ballistic deposition model also indicate that $\alpha < 0.4$. The presence of the intrinsic width as the main correction to the interface width scaling was considered to extrapolate the simulations data. We also obtain the estimates $S = 0.26 \pm 0.01$ and $Q = 0.134 \pm 0.015$ in the steady state regime of the etching model. Results for the BD model and of the BCSOS model, together with previous results for the RSOS model, suggest that the absolute value of S and the value of Q are universal, the sign of the skewness being the same of the parameter λ of the corresponding KPZ equation.

The above estimate intercepts the error bar of the roughness exponent of the RSOS model given by Marinari and co-workers [20], $\alpha = 0.393 \pm 0.003$. However, our central estimate is significantly lower than theirs, and the result for BD confirm this trend. On the other hand, our estimate is very near that by Colaioni and Moore, $\alpha \approx 0.38$, from renormalization methods [21]. Additional support to our conclusions was given by the independent calculation of

exponents z and β , contrary to recent simulation works on these lines [19,20], which were limited to the calculation of exponent α .

We believe that much more accurate estimates of α are difficult to be achieved with numerical simulations of this type of lattice model. However, we consider that this work provides a significant amount of numerical results indicating that the theoretically proposed value $\alpha = 0.4$ [18] is not valid, within the limits of the assumptions made about the form of finite-size scaling corrections. This result and the evidence of universality of the values of the skewness and the kurtosis may motivate further analytical (maybe also numerical) studies of the KPZ theory in $2 + 1$ dimensions.

-
- [1] *Frontiers in Surface and Interface Science*, edited by Charles B. Duke and E. Ward Plummer (Elsevier, Amsterdam, 2002).
[2] A.-L. Barabási and H. E. Stanley, *Fractal Concepts in Surface Growth* (Cambridge University Press, New York, 1995).
[3] J. Krug, *Adv. Phys.* **46**, 139 (1997).
[4] M. Kardar, G. Parisi and Y.-C. Zhang, *Phys. Rev. Lett.* **56** 889 (1986).
[5] F. Family and T. Vicsek, *J. Phys. A* **18** L75 (1985).
[6] J. M. Kim and J. M. Kosterlitz, *Phys. Rev. Lett.* **62** 2289 (1989).
[7] M. J. Vold, *J. Coll. Sci.* **14** (1959) 168; *J. Phys. Chem.* **63** 1608 (1959).
[8] P. Meakin, P. Ramanlal, L. M. Sander and R. C. Ball, *Phys. Rev. A* **34**, 5091 (1986).
[9] F. D. A. Aarão Reis, *Phys. Rev. E* **63** 56116 (2001).
[10] P. Devillard and H. E. Stanley, *Physica A* **160**, 298 (1989).
[11] D. Liu and M. Plischke, *Phys. Rev. B* **38**, 4781 (1988).
[12] B. M. Forrest and L. Tang, *J. Stat. Phys.* **60**, 181 (1990).
[13] T. Ala-Nissila, T. Hjelt, J. M. Kosterlitz and O. Venöläinen, *J. Stat. Phys.* **72**, 207 (1993).
[14] J. G. Amar and F. Family, *Phys. Rev. A* **41**, 3399 (1990).
[15] K. Moser, J. Kertész and D. E. Wolf, *Physica A* **178**, 215 (1991).
[16] M. Beccaria and G. Curci, *Phys. Rev. E* **50**, 4560 (1994).
[17] L. Giada, A. Giacometti, and M. Rossi, *Phys. Rev. E* **65**, 36134 (2002).
[18] M. Lässig, *Phys. Rev. Lett.* **80**, 2366 (1998).
[19] C.-S. Chin and M. den Nijs, *Phys. Rev. E* **59**, 2633 (1999).
[20] E. Marinari, A. Pagnani and G. Parisi, *J. Phys. A* **33**, 8181 (2000).
[21] F. Colaiori and M. A. Moore, *Phys. Rev. Lett.* **86**, 3946 (2001).
[22] Y. Shim and D. P. Landau, *Phys. Rev. E* **64**, 36110 (2001).
[23] B. A. Mello, A. S. Chaves and F. A. Oliveira, *Phys. Rev. E* **63**, 41113 (2001).
[24] J. G. Amar and F. Family, *Phys. Rev. Lett.* **64**, 543 (1990); **64**, 2334 (1990); J. Krug and H. Spohn, *ibid.* **64**, 2332 (1990); J. Kim, T. Ala-Nissila, and J. M. Kosterlitz, *ibid.* **64**, 2333 (1990).
[25] S.F. Edwards and D.R. Wilkinson, *Proc. R. Soc. London* **381**, 17 (1982).
[26] F. D. A. Aarão Reis, *Physica A* **316** 250 (2002).
[27] B. S. Costa, J. A. R. Euzébio, and F. D. A. Aarão Reis, *Physica A*, to appear (2003).
[28] J. Krug, P. Meakin, and T. Halpin-Healy, *Phys. Rev. A* **45** 638 (1992).
[29] J. Krug and P. Meakin, *J. Phys. A: Math. Gen.* **23** L987 (1990).
[30] D. E. Wolf and J. Kertész, *Europhys. Lett.* **4**, 651 (1987).
[31] J. Kertész and D. E. Wolf, *J. Phys. A* **21**, 747 (1988).
[32] E. Moro, *Phys. Rev. Lett.* **87**, 238303 (2001).

TABLE I. For each i in Eq. (11), are given: the values of the correction exponent Δ which provided the largest correlation coefficients r of fits of $\alpha_{(L,i)} \times L^{-\Delta}$ and the corresponding asymptotic α , the values of the slope B of the fits with fixed $\Delta = 0.55$ and the corresponding values of asymptotic α and of $B \ln i / (1 - i^\Delta)$.

i (Eq. 11)	Δ (largest r)	α (largest r)	B ($\Delta = 0.55$ fixed)	α ($\Delta = 0.55$ fixed)	$B \ln i / (1 - i^\Delta)$ ($\Delta = 0.55$ fixed)
2	0.55	0.384	0.472	0.384	0.705
2.56	0.50	0.383	0.434	0.381	0.603
3.125	0.6	0.383	0.553	0.385	0.723
4	0.65	0.381	0.545	0.383	0.661

FIG. 1. The growth rules of the model of Mello et al (original growth version). The arrows indicate the randomly chosen columns and the new particles are shown in gray.

FIG. 2. Steady state skewness of various models versus inverse lattice length: (a) etching model (in the growth version); (b) ballistic deposition; (c) BCSOS model with $K = 0.25$; (d) BCSOS model with $K = 1.0$. The solid lines in (a) and (c) are least squares fits of the data.

FIG. 3. Steady state velocities versus $1/L^{\alpha_{\parallel}}$, with $\alpha_{\parallel} = 1.24$, for: (a) etching model; (b) ballistic deposition model; (c) BCSOS model with $K = 0.25$; (d) BCSOS model with $K = 1.0$. Error bars are smaller than the size of the data points.

FIG. 4. Steady state kurtosis of various models versus inverse lattice length: (a) etching model; (b) ballistic deposition model (squares), BCSOS model with $K = 0.25$ (triangles) and BCSOS model with $K = 1.0$ (crosses). Error bars in (b) (not shown) are smaller than the size of the data points, except for BD in the largest lattice ($L = 1024$).

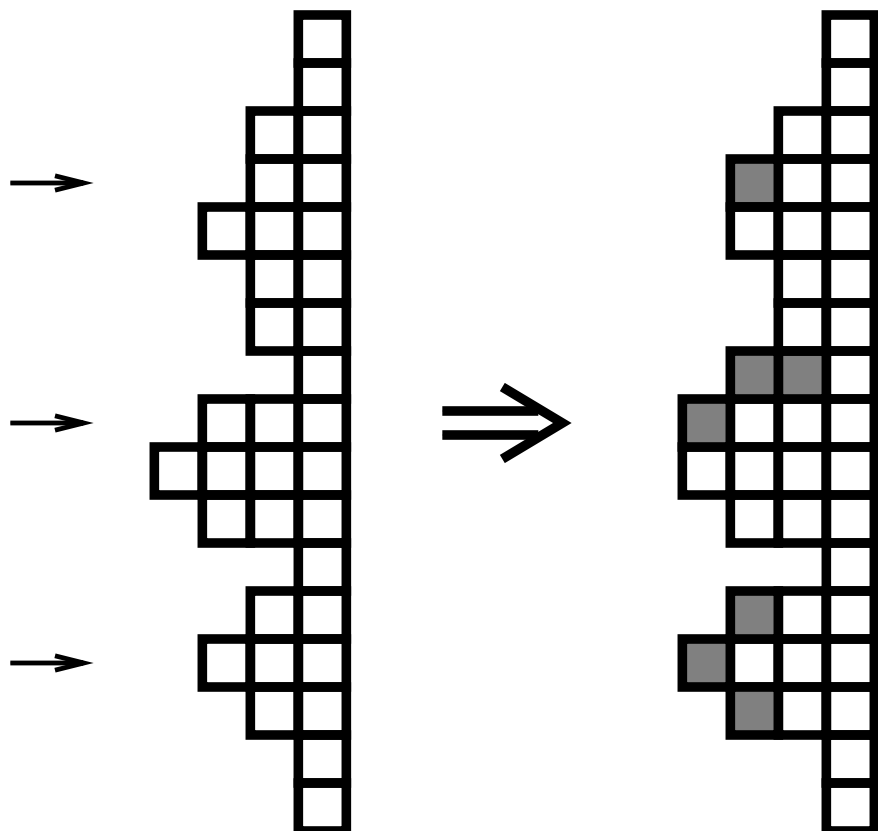
FIG. 5. Effective exponents $\alpha_{(L,2)}$ and $\alpha_{(L,4)}$ for the etching model versus $L^{-\Delta}$, with the exponents Δ that give the best linear fits for $i = 2$ and $i = 4$, respectively.

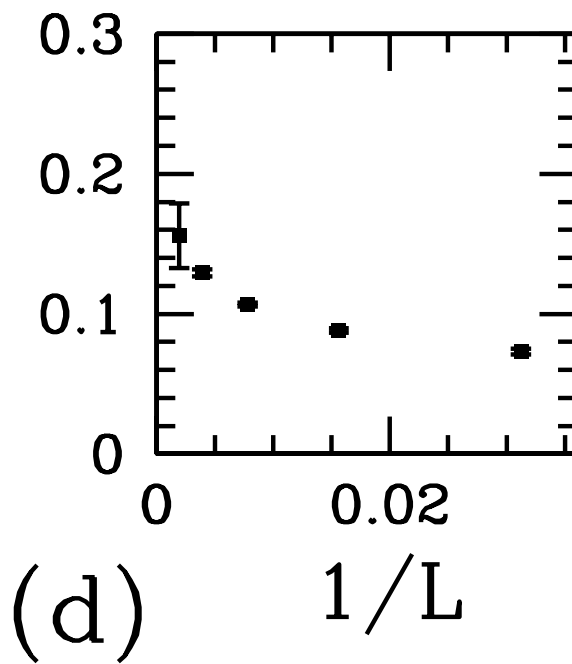
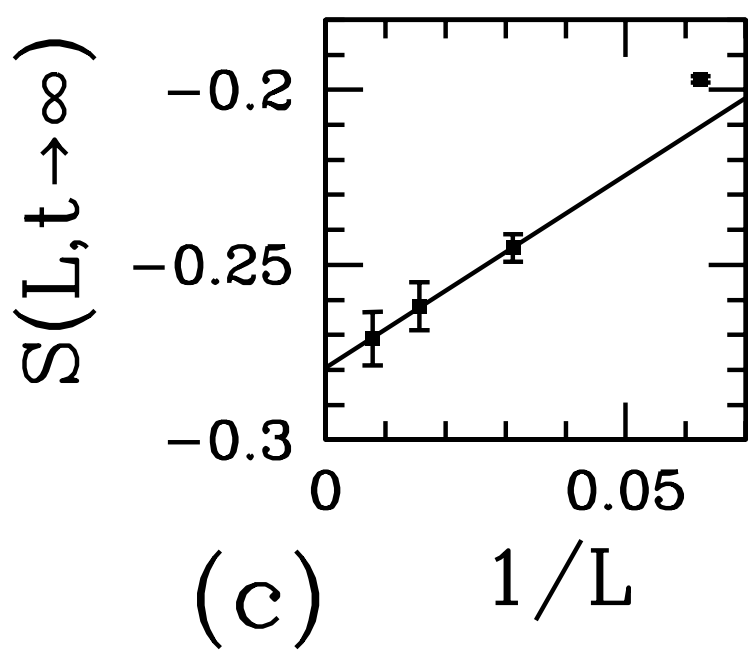
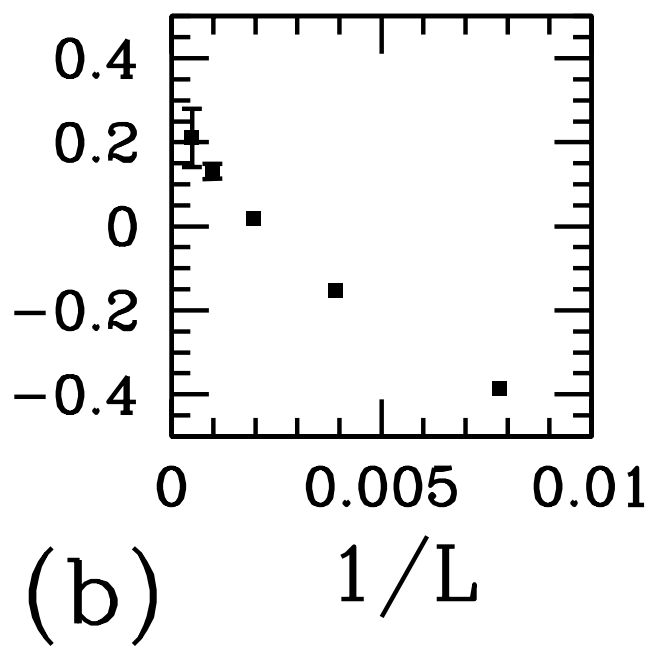
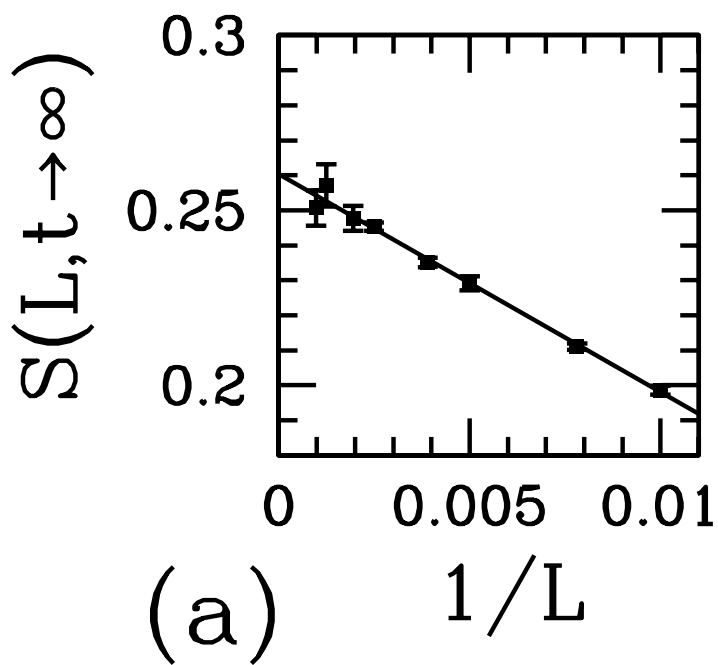
FIG. 6. Effective exponents $\alpha_L^{(I)}$ (from interface width) and $\alpha_L^{(I,4)}$ (from the fourth moment of the height distribution) for the etching model versus inverse lattice length.

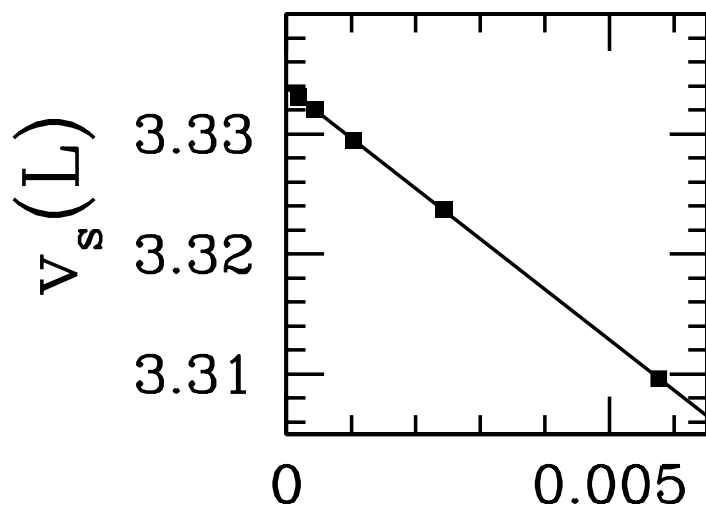
FIG. 7. Effective exponents $\alpha_L^{(I)}$ for the ballistic deposition model versus inverse lattice length.

FIG. 8. Effective exponents z_L for the etching model versus inverse lattice length. Relaxation times τ_0 were obtained with: (a) $k = 0.6$ and (b) $k = 0.8$ in Eq. (8).

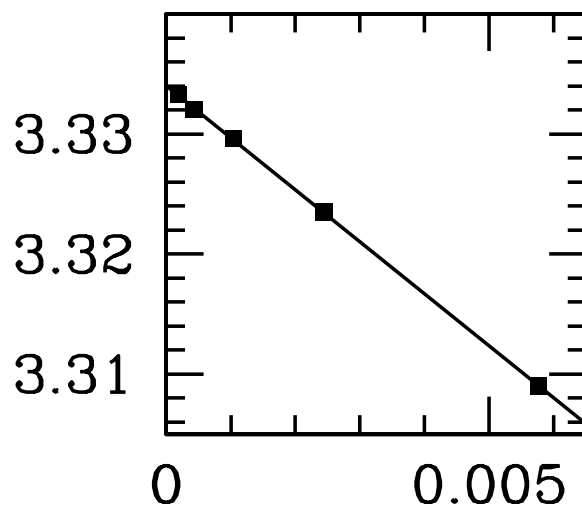
FIG. 9. Effective exponents β_L for the etching model versus inverse lattice length, obtained with minimum correlation coefficients $r_{min} = 0.9999$ (squares) and $r_{min} = 0.99995$ (triangles). Solid lines are least squares fits of each set of data ($200 \leq L \leq 1024$).



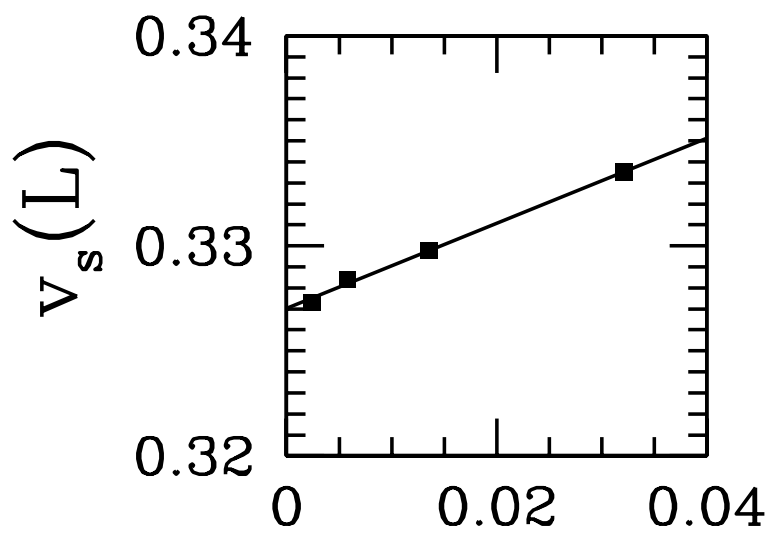




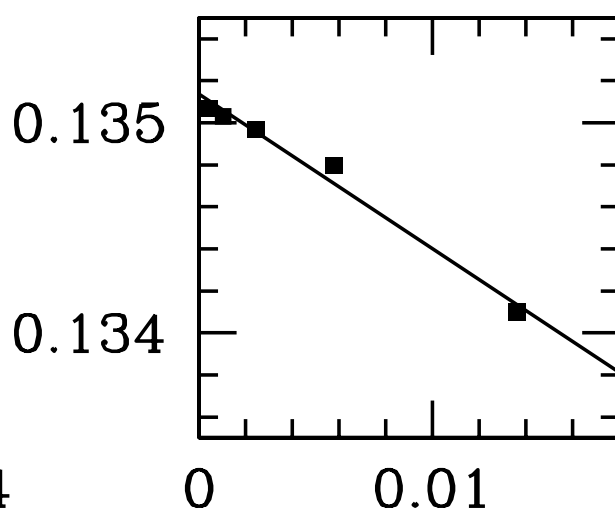
(a)



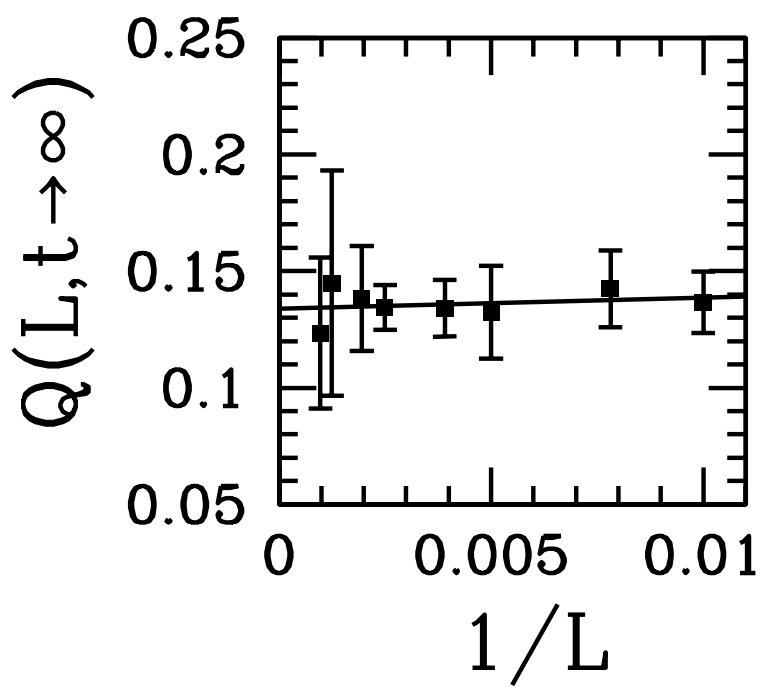
(b)



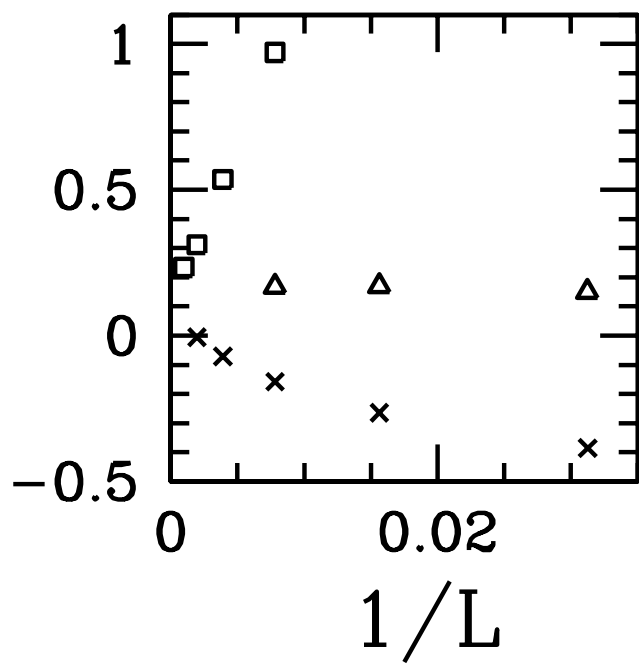
(c)



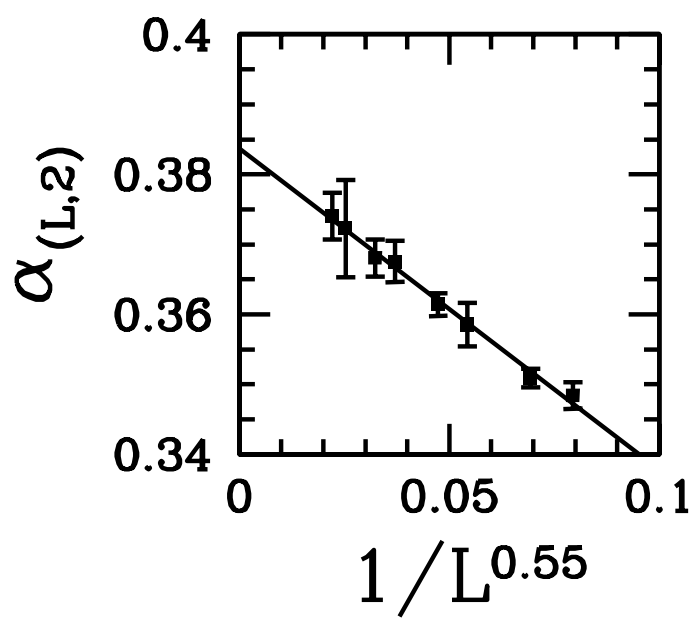
(d)



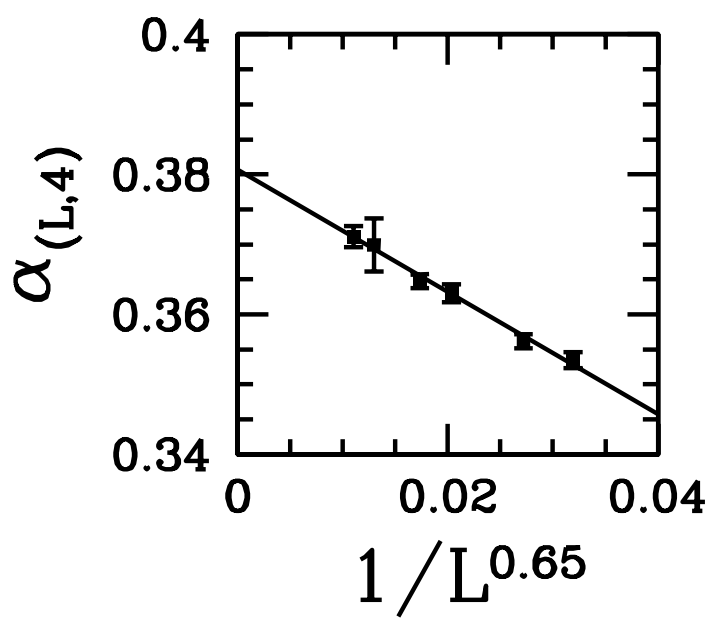
(a)



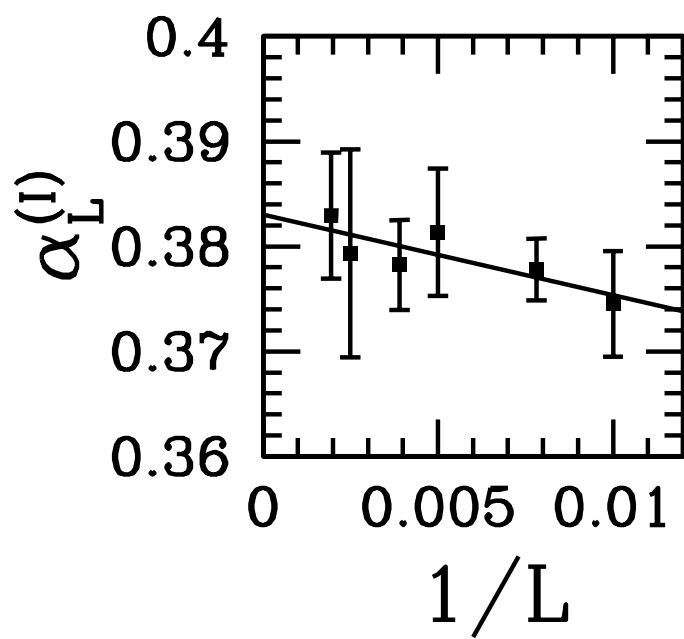
(b)



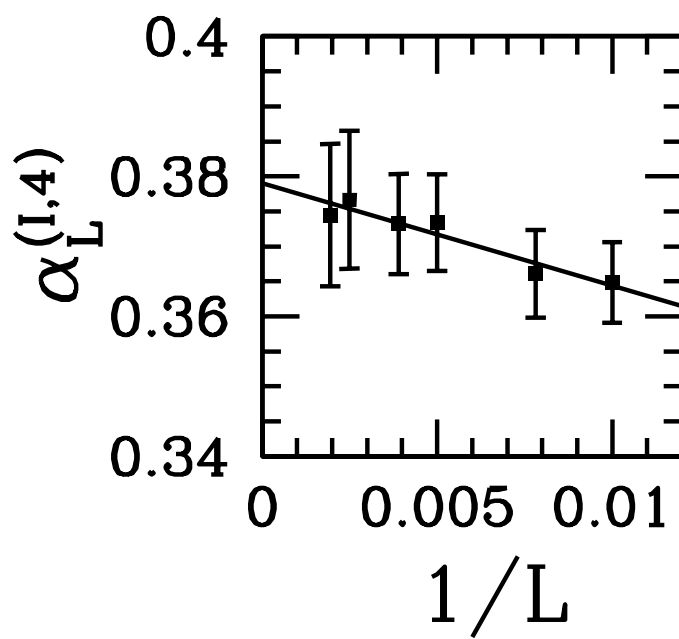
(a)



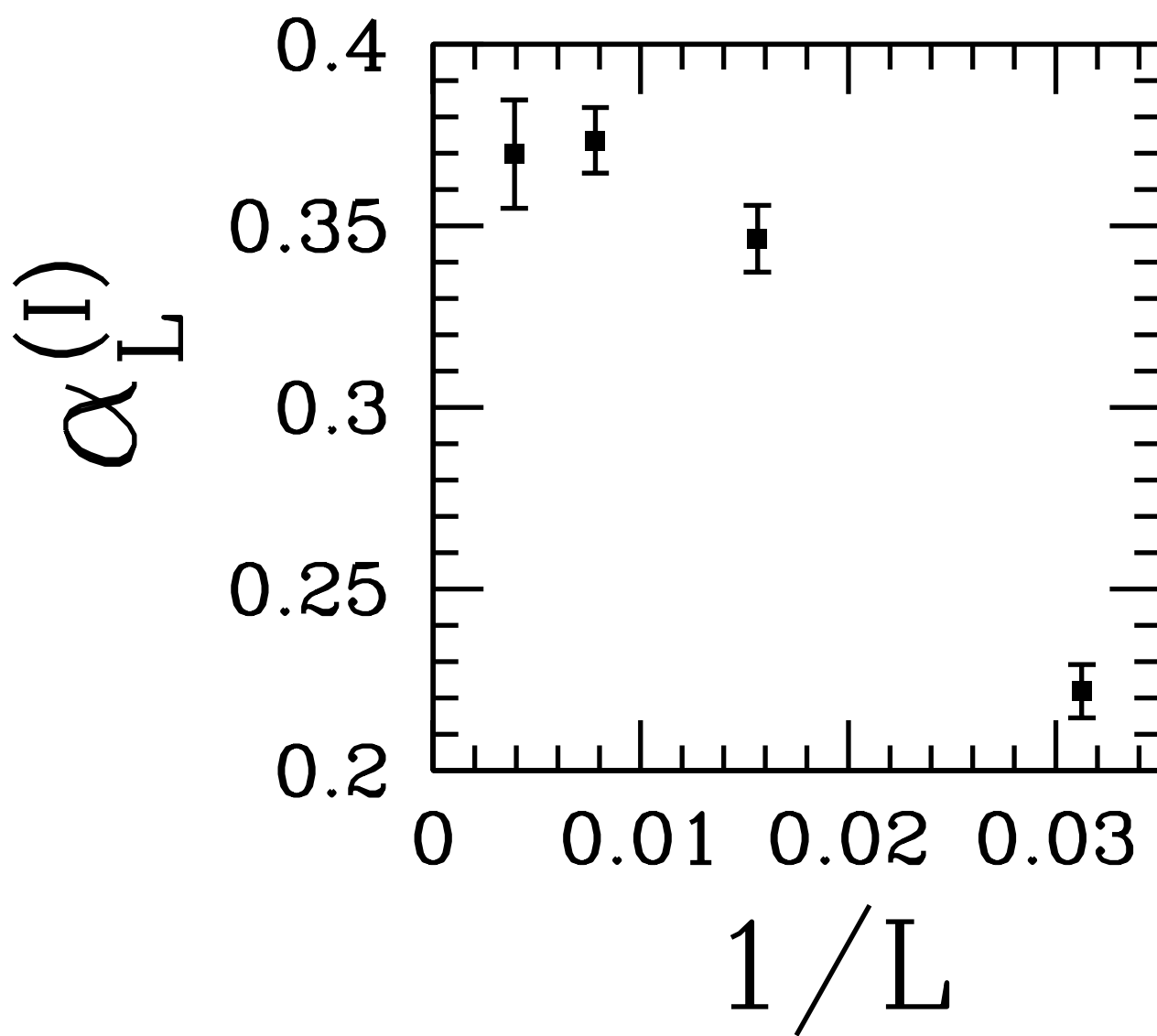
(b)

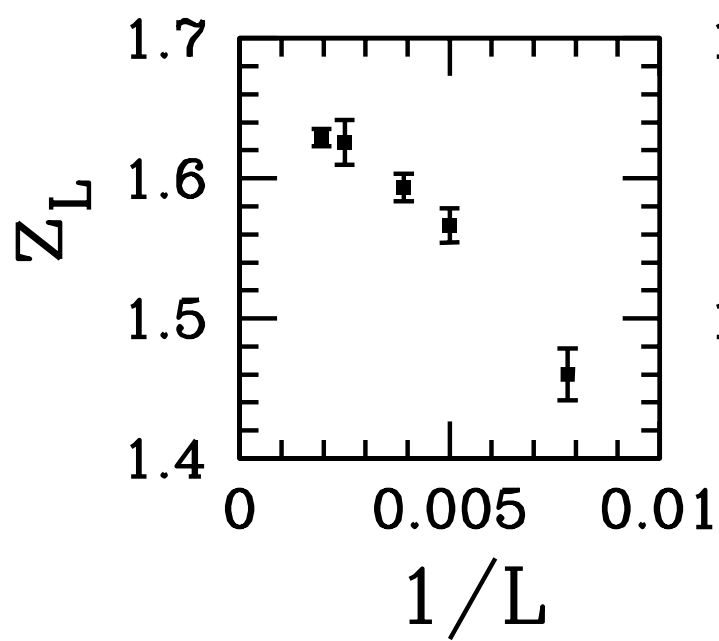


(a)

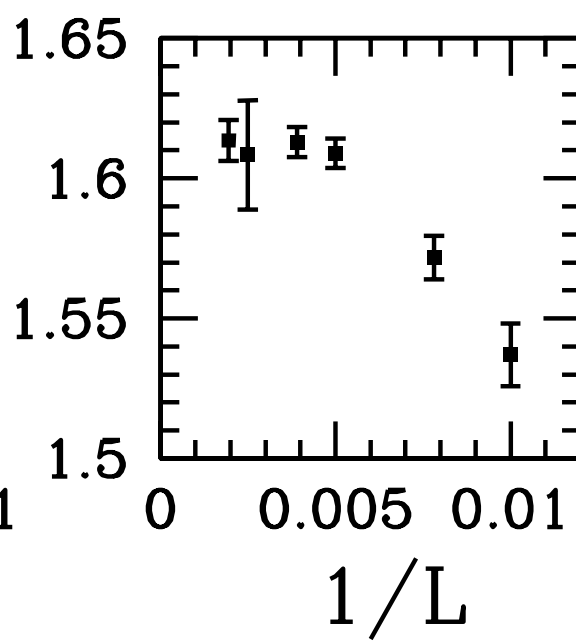


(b)





(a)



(b)

